Journal of Statistical Physics, Vol. 31, No. 3, 1983

What Can We Learn from Homoclinic Orbits in Chaotic Dynamics?

P. Gaspard[1] and G. Nicolis[1]

Received September 13, 1982

State diagrams of two model systems involving three variables are constructed. The parameter dependence of different forms of complex nonperiodic behavior, and particularly of homoclinic orbits, is analyzed. It is shown that the onset of homoclinicity is reflected by deep changes in the qualitative behavior of the system.

KEY WORDS: Bifurcation theory; homoclinic orbits; nonperiodic behavior; chaotic dynamics.

1. INTRODUCTION

One of the major complications encountered in current studies of transitions leading to chaotic dynamics is the *global character* of many of these phenomena. This leads to highly nonlinear evolution equations which, as a rule, remain intractable.

One can envisage two ways out of this difficulty. First, reduce some aspects of global dynamics to a local problem. And, second, even in the framework of a global description, find some features which characterize complex nonperiodic behavior as closely as possible. The basic idea behind the first attitude is the realization that many transitions which are global when one control parameter is varied become local when more than one such parameters are considered.[1] Thus, by studying certain codimension two bifurcations, it has been possible to show that complex nonperiodic behavior emerges both for autonomous[2] and for forced[3] systems.

[1] Faculté des Sciences de l'Université Libre de Bruxelles, Campus Plaine, CP 226, Bd du Triomphe, B1050 Bruxelles, Belgium.

0022-4715/83/0600-0499$03.00/0

The second point of view, namely, the characterization of complex behavior in the large, is a much more ambitious project. A beautiful example showing that in some cases such projects can nevertheless be fulfilled is Feigenbaum's discovery of universality of certain classes of mappings of the interval.[4,5] It is the purpose of the present paper to stress that an important role in organizing our information on complex behavior is the occurrence of *homoclinic orbits*, that is to say, infinite period orbits which are doubly asymptotic to a singular point of the saddle type as $t \to \pm\infty$. A similar point of view has been adopted in an interesting recent paper by Arneodo *et al.*,[6] which came to our knowledge after the present work was completed. Moreover, Afraimovitch *et al.*[7] have shown that homoclinic orbits shed some light on the origin and structure of the Lorenz attractor.

Homoclinic *points*, the intersections of stable and unstable manifolds of fixed points of discrete time mappings, are a familiar concept in global dynamics. Ever since their discovery by Poincaré and Birkhoff and their comprehensive study by Smale,[8] they have been regarded as "landmarks" signaling the onset of complex nonperiodic behavior. On the other hand, the role of homoclinic *orbits* in continuous time flows is much less explored since, for one thing, such orbits are structurally unstable.[9] It is only in the 1960s that some of their important and unsuspected features were discovered by Sil'nikov *et al.*[10,11] Of particular interest for our investigation is the following result.

Consider the three-variable system

$$\begin{aligned} \dot{x} &= \rho x - \omega y + P(x, y, z) \\ \dot{y} &= \omega x + \rho y + Q(x, y, z) \\ \dot{z} &= \lambda z + R(x, y, z) \end{aligned} \tag{1}$$

where P, Q, R are analytic functions vanishing together with their first derivatives at the origin $(0,0,0)$, which is a saddle-focus. We assume that one of the orbits, Γ_0, leaving the saddle-focus returns to it as $t \to \infty$. Then

(i) If $\lambda > -\rho > 0$ (or if $-\lambda > \rho > 0$) every neighborhood of Γ_0 contains a countable set of unstable periodic solutions of the saddle type.

(ii) There exists in a neighborhood of Γ_0 a subsystem of trajectories which display random behavior, in the sense that they are in one-to-one correspondence with a shift automorphism with an infinite number of symbols.

In view of these results, it is natural to conjecture that there should be a relation between homoclinic trajectories and complex nonperiodic behavior of the chaotic type. The search of homoclinic trajectories in model systems, their parameter dependence, and the characterization of chaotic

motions generated for nearby values of parameters, is the principal goal of the present work.

In Section 2, we consider a three-variable model proposed by Rössler as one of the prototypes of chaotic behavior.[12] We determine the singular points and their stability properties, and show that around either of these points the evolution can be cast in the Sil'nikov form [Eq. (1)] for certain ranges of parameter values. Section 3 is devoted to the nonlinear behavior: limit cycles, Feigenbaum sequences, chaos, and homoclinic orbits. Specifically, we show that the system admits such orbits and we construct state diagrams determining their location in a two-parameter space. We also comment on the type of effects that can occur on crossing the parameter values for which a homoclinic orbit exists, and particularly on the mixing properties of the trajectories on the attractor in the vicinity of such orbits. In Section 4 we repeat the calculations for a new three-variable model whose main interest is to be compatible with mass action kinetics.[13] Here we find again homoclinic trajectories, in the vicinity of which chaotic solutions obey some interesting rules. In the final Section 5, we discuss the implications of the results.

2. RÖSSLER'S MODEL—SINGULAR POINTS AND LINEAR STABILITY ANALYSIS

We consider the three-variable system[12]

$$\begin{aligned} \dot{x} &= -y - z \\ \dot{y} &= x + ay \\ \dot{z} &= bx - cx + xz \end{aligned} \tag{2}$$

and limit ourselves to the cases in which the parameters a, b, and c are positive.

The system possesses two singular points:

$$x_1 = y_1 = z_1 = 0 \tag{3a}$$

and

$$x_2 = c - ab, \qquad y_2 = b - \frac{c}{a}, \qquad z_2 = \frac{c}{a} - b \tag{3b}$$

Linear stability analysis shows that both states can be, under certain conditions, saddle-foci as required by Sil'nikov's theorem. Specifically, we obtain the following types of behavior.

(i) *For point* (x_1, y_1, z_1): The characteristic equation takes the form

$$\lambda^3 + (c - a)\lambda^2 + (1 + b - ac)\lambda + c - ab = 0 \tag{4}$$

The locus of points in parameter space for which the roots are of the form $(i\omega, -i\omega, \lambda)$ is

$$a_{\pm} = \frac{(1+c^2) \pm \left[(1+c^2)^2 - 4bc^2\right]^{1/2}}{2c} \tag{5}$$

On the other hand, the locus of points for which the roots are $(\lambda_1, \lambda_2, 0)$ is

$$a = \frac{c}{b} \tag{6}$$

(ii) *For point* (x_2, y_2, z_2): The characteristic equation takes the form

$$\lambda^3 + a(b-1)\lambda^2 + \left(1 + \frac{c}{a} - a^2 b\right)\lambda + ab - c = 0 \tag{7}$$

The locus of points for which the roots are $(i\omega, -i\omega, \lambda)$ is

$$c = \frac{a}{b} + (b-1)a^3 \tag{8}$$

and the locus for which the roots are $(\lambda_1, \lambda_2, 0)$ is

$$a = \frac{c}{b} \tag{9}$$

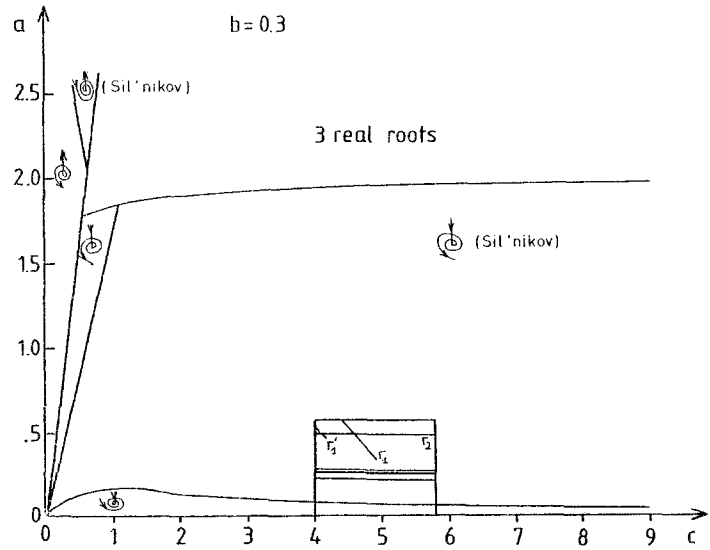

Fig. 1. State diagram in the space of parameters (a, c) for Rössler's model, obtained from the analysis of the characteristic equation around singular point (x_1, y_1, z_1). The nature of the characteristic roots is illustrated schematically in each part of the diagram, and the regions in which the singular point is a saddle-focus satisfying condition (i) of Sil'nikov's theorem are indicated explicitly. The framed part is magnified in Fig. 3, where the nonlinear behavior is analyzed.

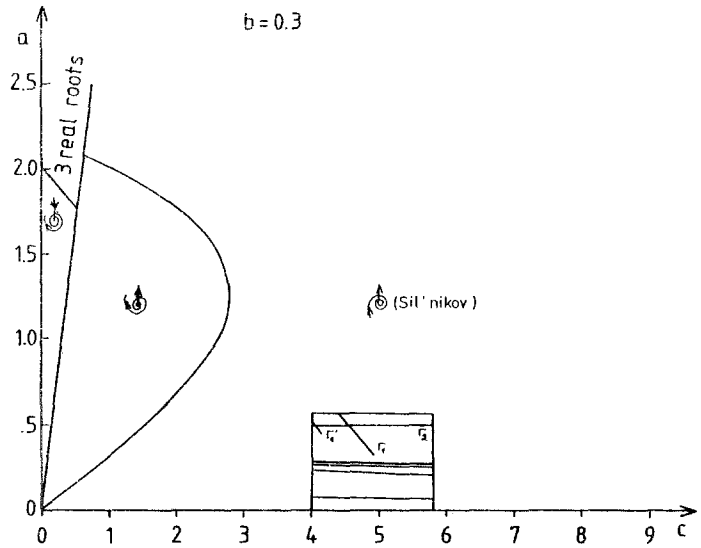

Fig. 2. Same as Fig. 1, except that the characteristic equation analyzed is around the singular point (x_2, y_2, z_2).

Figures 1 and 2 summarize the information obtained from linear stability, in the form of "state diagrams" in the space of a and c, keeping b fixed to the value $b = 0.3$.

An interesting limiting case arises when the two singular points merge. From Eqs. (3a)–(3b) it is clear that this happens when $c = ab$.

Moreover, Eqs. (6) or (9) show that in this case one of the roots of the characteristic equation is zero. The remaining two roots are given by the relation

$$\lambda = \frac{a(1-b) \pm \left[a^2(b+1)^2 - 4(b+1)\right]^{1/2}}{2} \tag{10}$$

It follows that when

$$a^2(b+1) \leqslant 4 \tag{11}$$

the eigenvalues will be complex conjugate, and that the sign of their real part will be negative or positive according as $b > 1$ or $b < 1$. When $b = 1$, inequality (11) is satisfied for $0 \leqslant a \leqslant \sqrt{2}$. On this segment of the parameter space spanned by a, b one will have therefore a degenerate situation corresponding to eigenvalues $(i\omega, -i\omega, 0)$. By slightly varying the parameters from this special situation, one can hope to approach the behavior of

Eqs. (2) by perturbation theory. We come back to this problem in the discussion.

3. NONLINEAR BEHAVIOR—HOMOCLINIC ORBITS

We have carried out an extensive study of the nonlinear behavior of Eqs. (2) in parameter space, keeping $b = 0.3$ and varying a and c in the interval $0 \leqslant a \leqslant 0.55$, $4 \leqslant c \leqslant 5.8$. Different aspects of the parameter dependence of the model have been reported recently in an interesting paper by Fraser and Kapral.[14] The integration method followed was an im-

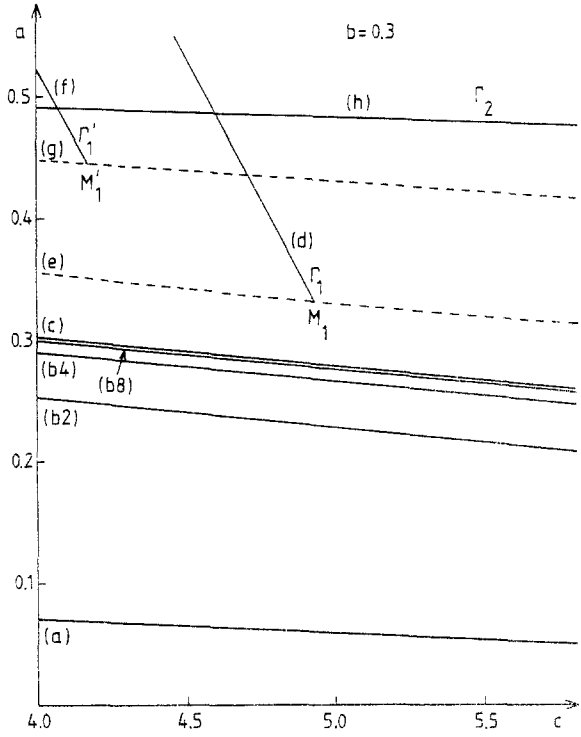

Fig. 3. Nonlinear behavior and transitions in Rössler's model in the space of parameters (a, c). Curve (a): line of Hopf bifurcations around singular point (x_1, y_1, z_2); curves (b2)–(b8): lines of period doubling bifurcations; curve (c): line delimiting onset of chaotic behavior; curves (d), (f): lines along which two homoclinic orbits Γ_1, Γ_1' associated to (x_1, y_1, z_1) exist; curve (e): transition line between "spiral"- and "screw"-type chaos conditioned by homoclinic orbit Γ_1, and reflected by a jump in the return time plot (Fig. 6); curve (g): line indicating similar transition conditioned by homoclinic orbit Γ_1'; curve (h): line along which a homoclinic orbit Γ_2 associated with (x_2, y_2, z_2) exists.

proved Euler method with an $O(h^3)$ error on the step h. We here summarize the main results.

(i) *Hopf bifurcation*: In the above-defined range of values of a and c relation (8) is never satisfied, but relation (5) can be satisfied for a_-. It follows that, for a given value of c, a Hopf bifurcation will take place from the singular point (x_1, y_1, x_1) as a increases beyond the value a_-. Curve (a) of Fig. 3 describes the transition locus. Note the existence of a large region within $a \geqslant a_-$ in which the third real eigenvalue exceeds in absolute value the real part of the complex conjugate eigenvalues. In particular, from Eq. (4) it is seen that this is always so near a_-, as long as $c > a$. In other words, one of the requirements for the validity of Sil'nikov's theorem can be readily satisfied.

The limit cycle resulting from the Hopf bifurcation can be constructed analytically and shown to be attractive in the domain of parameter values considered in Fig. 3. Details of the computations are given in Ref. 13.

(ii) *Period doubling sequence*: For values of a well above a_-, period doubling bifurcations are detected which are in qualitative agreement with Feigenbaum's scenario.[4,5] Curves (b2)–(b8) of Fig. 3 describe the transition loci in parameter space. They have been determined numerically by studying the Poincaré map of the flow on the plane $x = 0$.

(iii) *Chaotic behavior*: For still larger values of a [beyond curve (c) of Fig. 3], chaotic behavior is observed in a large domain of the parameter values. Two characteristic attractors, corresponding to $(a = 0.32,\ c = 4.5)$ and $(a = 0.38,\ c = 4.5)$ are shown in Figs. 4a and 4b, respectively. Their structure is markedly different and suggests that, somewhere along the interval $0.32 < a < 0.38$, a transition between "spiral"-type and "screw"-type chaos should take place.[6,12] As it turns out *this transition reflects the existence of homoclinic orbits in the system*. We turn to this point presently.

(iv) *Homoclinic orbits*: As pointed out in Section 2, in certain regions of the parameter space both singular points of the system can satisfy the conditions required by Sil'nikov's theorem. It is therefore natural to seek homoclinic trajectories in this range.

Consider first the singular point (x_1, y_1, z_1). For the range of parameter values given in Fig. 3, this point behaves as a saddle-focus with a one-dimensional stable manifold and a two-dimensional unstable manifold. To determine a homoclinic trajectory we studied the intersections of the unstable manifold with a plane transversal to the local stable manifold, which are generated by several trajectories starting from the (local) unstable manifold near the singular point. By varying one of the parameters at a time, we could determine, by interpolation, the value at which the unstable manifold contains the stable one. Curve (d) of Fig. 3 gives the parameter values for which this homoclinic trajectory Γ_1 exists. Its phase space

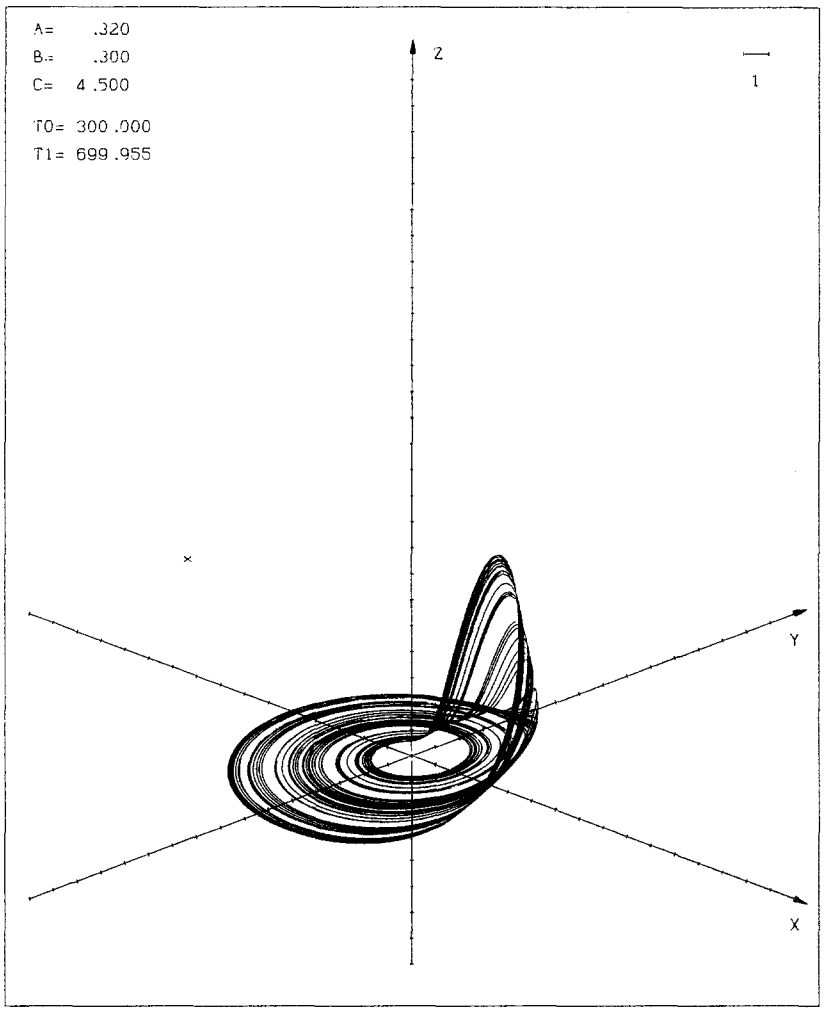

Fig. 4. (a) Nonperiodic attractor of the spiral type in Rössler's model, obtained for the parameter values indicated and for initial condition $x = y = z = 1$. T_0, T_1: beginning and end of integration interval, during which the attractor is traced; $\times$: singular point (x_2, y_2, z_2); $\vdash\!\!\dashv$: unit interval along the axes.

portrait for $a = 0.38$, $b = 0.3$, $c = 4.82$ is given in Fig. 5. The attractor containing this trajectory has a phase portrait quite similar to that of Fig. 4b. Curve (d) ends at a point M_1. This fact is caused by the folding of the unstable manifold, which can be seen from Figs. 4a or 4b. It may thus be expected that curve (d) will also be folded near point M_1, and that on

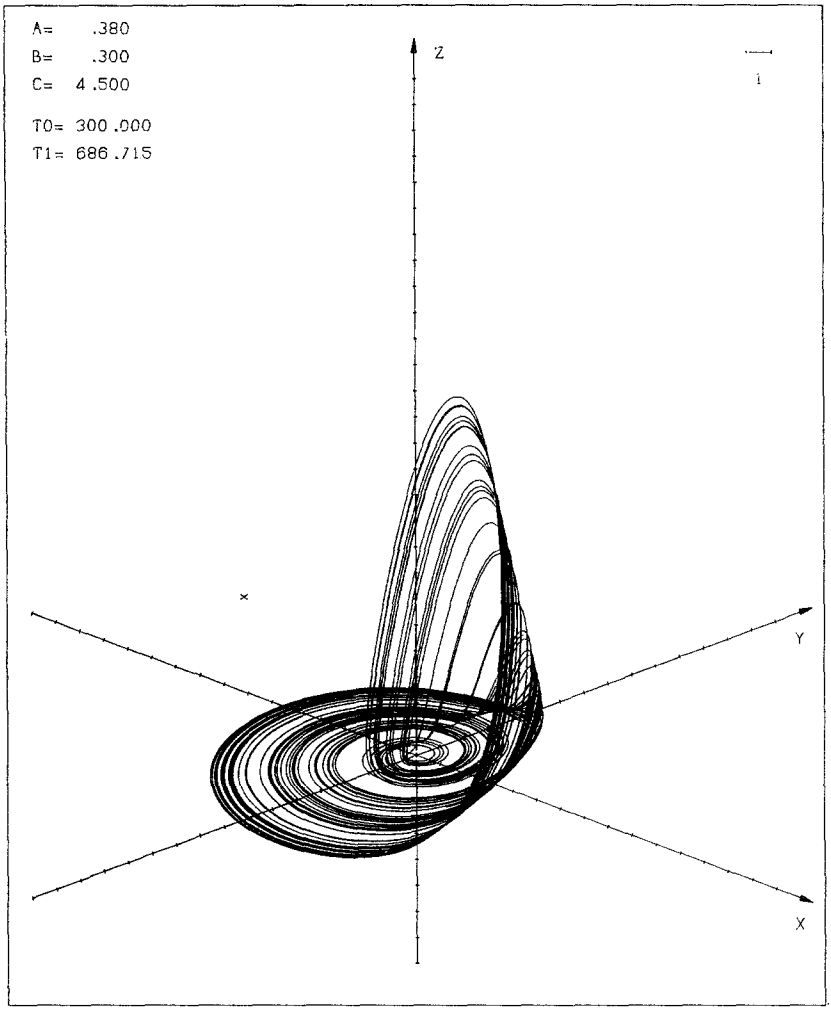

Fig. 4 (continued). (b) Nonperiodic attractor of the screw type in Rössler's model obtained for the parameter values indicated and for otherwise similar conditions as in Fig. 4a.

crossing this curve transversally along a path slightly above M_1, one will encounter in a very narrow interval of values of parameter c two flows containing a homoclinic orbit.

Curve (e) of Fig. 3, the frontier between spiral-type chaos and screw-type chaos also emanates from point M_1. It can be determined by using the following criterion. The successive iterates x_n of the flow on the plane ($y = 0$, $x < 0$, $z < 1$), as well as the times t_n needed by the trajectory

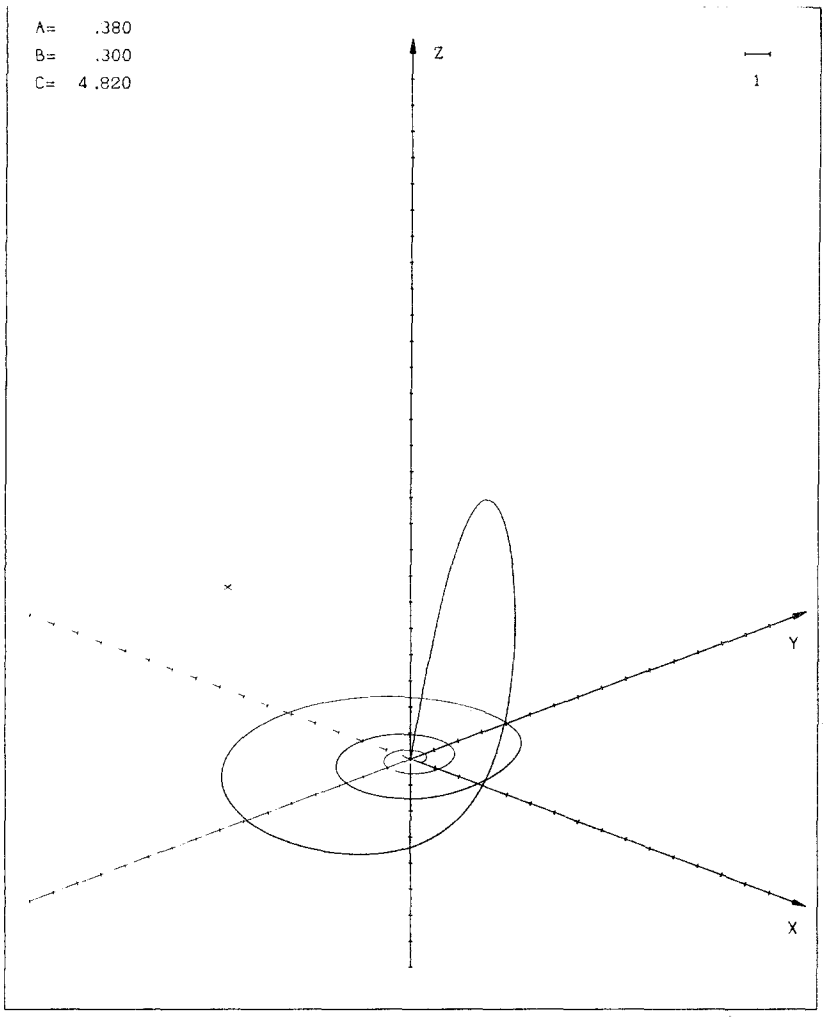

Fig. 5. Homoclinic orbit Γ_1 for Rössler's model around singular point (x_1, y_1, z_1). Parameter values are indicated on the figure. Eigenvalues around that point are given by $(\rho \pm i\omega, \lambda)$, where $\rho \simeq 0.1597$, $\omega \simeq 0.9815$, $\lambda \simeq -4.7594$. Initial condition lies on the local unstable manifold at a distance of about 0.47 from (x_1, y_1, z_1), and on plane $y = 0$.

starting at x_n to cross again this plane, are computed. The graphs of the functions $(-x_n \to -x_{n+1}), (-x_n \to t_n)$ are plotted in Figs. 6a and 6b, for the attractors depicted in Figs. 4a and 4b, respectively. The difference is striking, especially in the return time plots: here the jump observed in the screw-type chaos implies that the spreading of nearby initial conditions on

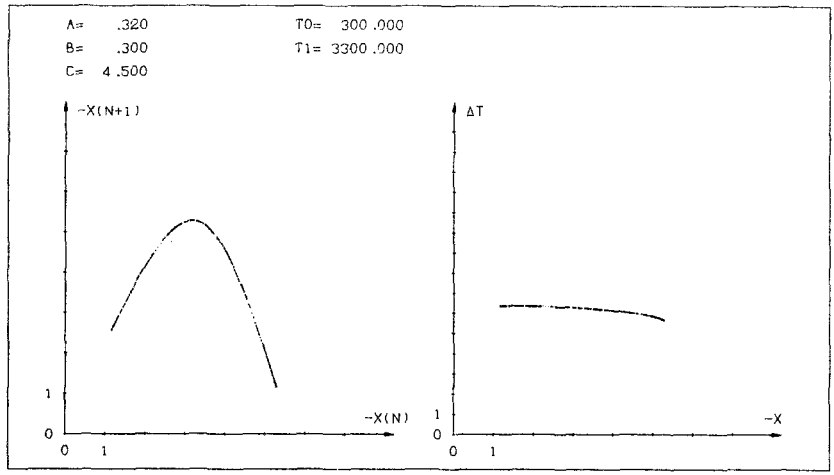

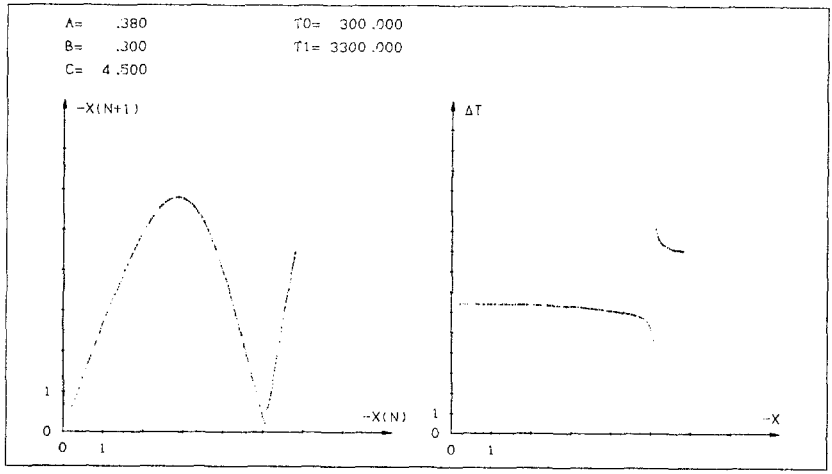

Fig. 6. (a) Left: successive iterates of the flow generated by the attractor of Fig. 4a on the plane ($y = 0$, $x < 0$, $z < 1$). Right: return time plot obtained under the same conditions. Parameter values and integration time interval are indicated on the figure. (b) Similar plots for the flow generated by the attractor of Fig. 4b.

the attractor by the flow is more efficient than for spiral-type chaos.[15] This can be used therefore as a criterion for locating curve (e), which delimits these two different types of motion. Note that the time dependence of the variables undergoes also a qualitative change when curve (e) is crossed. Specifically, in the spiral-type chaos the times at which one has

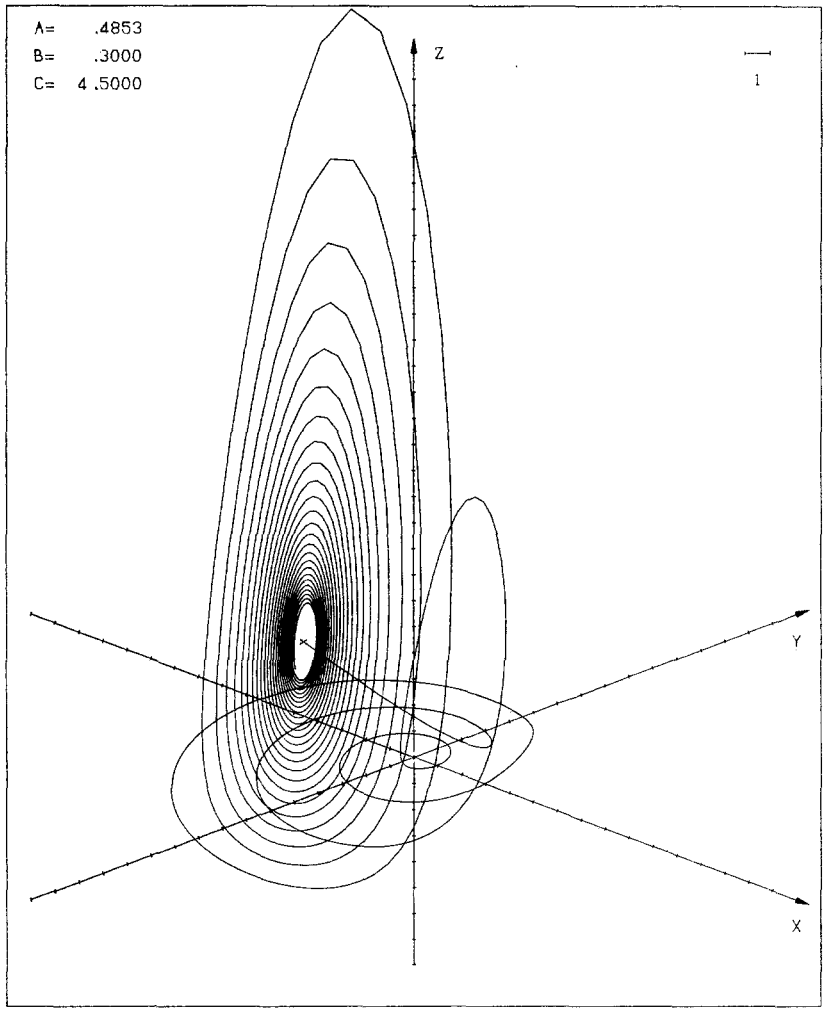

Fig. 7. Homoclinic orbit Γ_2 for Rössler's model around singular point (x_2, y_2, z_2). Parameter values are indicated on the figure. Eigenvalues around that point are given by $(\rho \pm i\omega, \lambda)$, where $\rho \simeq -0.0428$, $\omega \simeq 3.1994$, $\lambda \simeq 0.4253$. Initial condition lies on the local unstable manifold at a distance of about 0.14 from the singular point.

extrema of the oscillations are distributed fairly regularly, whereas in the screw type they form a random sequence.

The above remarks substantiate the role of homoclinic orbits in the onset of chaotic motion displaying strong mixing properties on the attractor.

Curve (f) of Fig. 3 is the locus in parameter space for which another homoclinic orbit, Γ_1', associated with the same singular point (x_1, y_1, z_1) exists. Its existence reflects another transition which takes place along curve (g) between chaotic attractors for which the return time plot presents one jump and those for which it contains two successive jumps (and thus implies that a longer time is required). The same remarks as above about the end point M_1' and the folding of the curve (f) also hold here.

It should be pointed out that not all the attractors in the part of Fig. 3 above curve (c) are necessarily chaotic, even if a homoclinic orbit exists in the flow. For instance, for the parameter values ($a = 0.4$, $c = 4.7737$) on curve (d) we found an attracting periodic motion, located in phase space away from the vicinity of the homoclinic orbit.

We turn now to the singular point (x_2, y_2, z_2). In the parameter range studied in Fig. 3, this point is a saddle-focus with a two-dimensional stable manifold and a one-dimensional unstable manifold. A homoclinic trajectory Γ_2 associated with it can be determined by the same method as above. Its locus in parameter space is given by curve (h) of Fig. 3, whereas a phase-space plot is given in Fig. 7. A characteristic feature of Γ_2 is the nonexistence of an attractor in this range of parameter space. A trajectory starting near Γ_2 would, typically, approach the vicinity of the singular point, spiral around it, and eventually diverge. The absence of (attracting) chaos under conditions for which Γ_2 exists has also been pointed out by Arneodo *et al.* in Ref. 6.

From the existence of Γ_2 it can be proven analytically[13] that if curve (h) is approached transversally from below, a sequence of flows possessing another class of homoclinic orbits associated with (x_2, y_2, z_2) and accumulating exponentially to (h) is encountered. In view of the complexity of these phenomena, the exact frontier of attractivity could not be determined easily. In any case, from the above results we are entitled to conclude that homoclinic trajectories play here a clear-cut role, as they are associated with bifurcations leading to the loss of asymptotic stability of the Rössler attractor.

4. A MODEL DERIVING FROM MASS ACTION KINETICS

Rössler's model, Eq. (2), admits positive as well as negative solutions. As it stands, therefore, it cannot be regarded as a model of chaotic behavior in chemical or population dynamical evolution equations. For this reason we present, in this section, a model which obeys mass-action kinetics and is also capable of generating complex nonperiodic behavior.

We consider the reaction scheme

$$\begin{cases} A_1 + X \to 2X \\ A_2 + 2X \to 3X \\ X + Y \to P_1 + Y \\ X + Z \to P_2 + Z \end{cases}$$

$$\begin{cases} A_3 + X + Y \to X + 2Y \\ A_4 + Z + Y \to Z + 2Y \\ Y \to P_3 \end{cases} \tag{12}$$

$$\begin{cases} A_5 + X \to X + Z \\ A_6 + 2Z \to 3Z \\ 3Z \to P_4 \\ Z \to P_5 \end{cases}$$

On suitably scaling the variables and the parameters one can easily verify that the rate equations can be cast in the form

$$\begin{aligned} \dot{x} &= x(dx - fy - z + g) \\ \dot{y} &= y(x + sz - l) \\ \dot{z} &= \frac{1}{\epsilon}(x - az^3 + bz^2 - cz) \end{aligned} \tag{13}$$

where all parameters are positive, all but ϵ are of $O(1)$, and $\epsilon \ll 1$. Note the existence of a fast time scale in the model, related to the smallness of ϵ.

All steady states of the system lie on the "slow manifold"

$$x = az^3 - bz^2 + cz \tag{14}$$

It can be easily checked that for

$$\frac{1}{4} < \frac{ac}{b^2} < \frac{1}{3} \tag{15}$$

this curve is S-shaped and crosses the z axis only at $z = 0$.

Two possible sets of steady states are solutions of the following algebraic equations:

$$\begin{aligned} x_1 = l - sz_1, \qquad y_1 &= \frac{1}{f}(dx_1 - z_1 + g) \\ az_1^3 - bz_1^2 + (c + s)z_1 - l &= 0 \end{aligned} \tag{16a}$$

and

$$\begin{aligned} y_2 = 0, \qquad z_2 &= dx_2 + g \\ x_2 &= az_2^3 - bz_2^2 + cz_2 \end{aligned} \tag{16b}$$

Moreover, the origin

$$x_3 = y_3 = z_3 = 0 \tag{16c}$$

is always a steady state.

In order to study that exact location of the above steady states and their stability, it will be convenient to fix the values of all but a few of the parameters. We carried out two series of investigations, corresponding to

$$\begin{gathered} a = 0.5, \quad b = 3, \quad c = 5, \quad \epsilon = 0.01 \\ f = 0.5, \quad g = 0.6, \quad s = 0, \quad l = 1.5 \\ 0.3 \leqslant d \leqslant 0.6 \end{gathered} \tag{17a}$$

and

$$\begin{gathered} a = 0.5, \quad b = 3, \quad c = 5, \quad \epsilon = 0.01 \\ f = 0.5, \quad g = 0.6, \quad s = 0.3 \\ 0.3 \leqslant d \leqslant 0.55, \quad 1.2 \leqslant l \leqslant 1.5 \end{gathered} \tag{17b}$$

For all these values, the origin (x_3, y_3, z_3) is unstable and Eqs. (16b) admit two positive solutions which turn out to be unstable. On the other hand, Eqs. (16a) may admit up to three solutions, but only one of them is positive and thus physically acceptable. For a wide range of parameter values this state behaves as a saddle-focus, with a one-dimensional stable manifold, satisfying the conditions required by Sil'nikov's theorem. The locus in parameter space for which the characteristic roots are $(i\omega, -i\omega, \lambda)$ is given by

$$d \equiv d_c = \frac{1}{3az_1^2 - 2bz_1 + c} + O(\epsilon) \tag{18}$$

We turn now to the nonlinear behavior of the system.

(i) *The parameter values vary according to Eq.* (17a): Figure 8 describes the qualitative behavior. The first transition is a Hopf bifurcation which takes place when d is increased beyond the threshold given by Eq. (18). The resulting limit cycle becomes in turn unstable for $d \simeq 0.47$. A complex sequence of transitions takes then place. Let M^p denote a periodic attractor whereby the system performs p turns around the singular point and visits M times the upper part of the manifold, Eq. (14). Furthermore let $(M^p, N^q, \ldots)$ denote a nonperiodic attractor whereby the system performs, in an apparently random manner, a succession of motions of the type M^p, N^q, etc. One can then show that, for parameter values beyond the instability of the limit cycle, the system goes successively through periodic and nonperiodic attracting regimes of the type defined above.

A comment on the numerical integration is here in order. Owing to the presence of the smallness factor ϵ, the system of Eqs. (13) is stiff. A simple

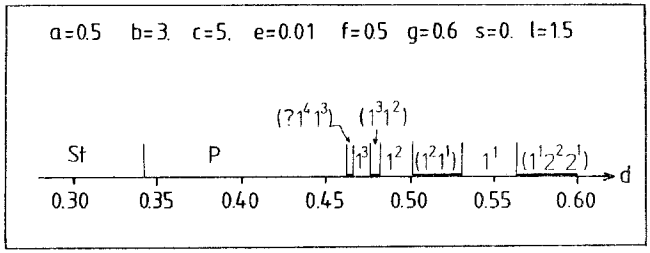

Fig. 8. Transitions taking place for model (12) as the parameter d varies in the interval $0.3 \leqslant d \leqslant 0.6$ and the other parameters are fixed according to Eq. (17a). St, stable steady state; P, stable periodic state bifurcating from St. Subsequently a succession of nonperiodic motions of the type $(M^p, N^q, \ldots)$ interrupted by windows of periodic motions of the type M^p is observed.

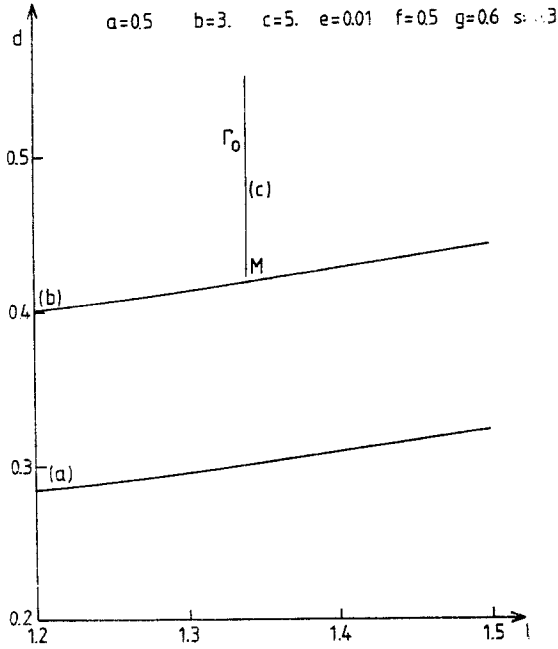

Fig. 9. Transitions taking place for model (12) in the space of the two parameters d and l [see Eq. (17b)]. Curve (a): line of Hopf bifurcations; curve (b): line of loss of stability of the limit cycle; curve (c): line along which a homoclinic orbit Γ_0, associated with (x_1, y_1, z_1) exists.

second-order integration method as described in the preceding section yields therefore instabilities. One way to avoid this[13] is to normalize the velocity field, **V** and study the phase portrait of the vector field evolving according to

$$\dot{\mathbf{X}} = \frac{\mathbf{V}}{\|\mathbf{V}\|} \tag{19}$$

where $\|\mathbf{V}\| = (\sum_i V_i^2)^{1/2}$ and each V_i is given by the right-hand sides of Eqs.

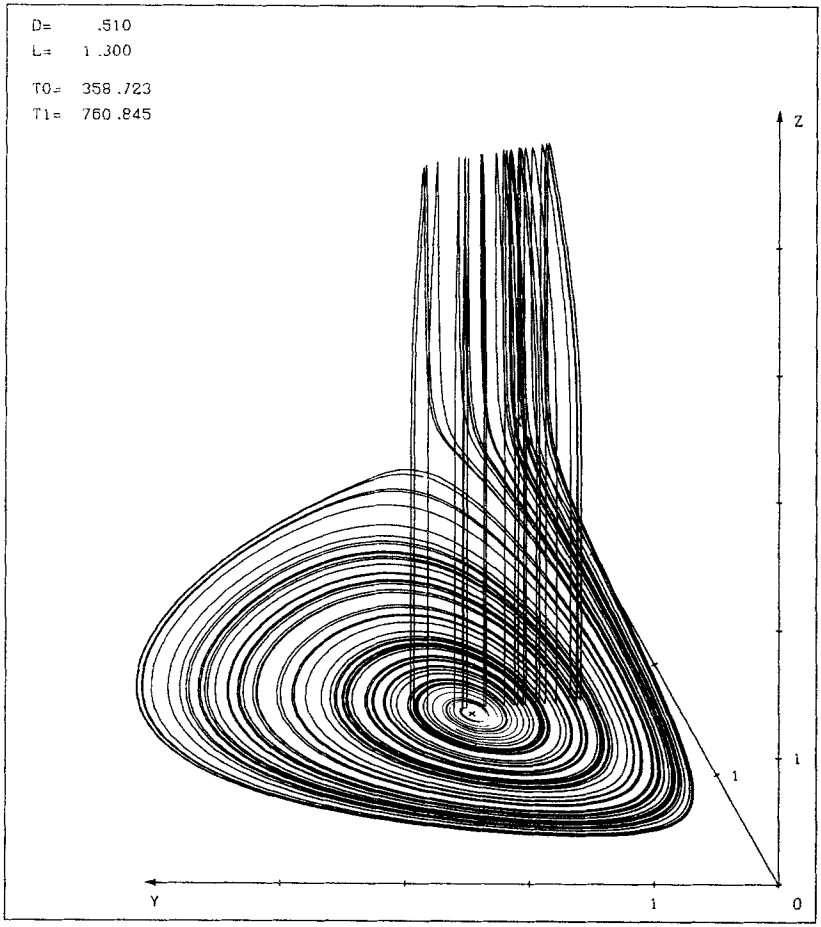

Fig. 10. Nonperiodic attractor emerging beyond line (b) of Fig. 9 for $d = 0.510$, $l = 1.300$, and other parameter values given by Eq. (17b). Initial condition: $x = y = z = 1$; ×: singular point (x_1, y_1, z_1).

(13). This preserves the phase portrait of the original system and amounts to introducing a "local" time scale in the system, which varies along the trajectories.

(ii) *The parameter values vary according to Eq.* (17b): Figure 9 describes the situation. In the parameter space spanned by d and l, a line of Hopf bifurcation is first encountered as d is increased [curve (a)]. Subsequently the limit cycle loses its stability [curve (b)], and a variety of

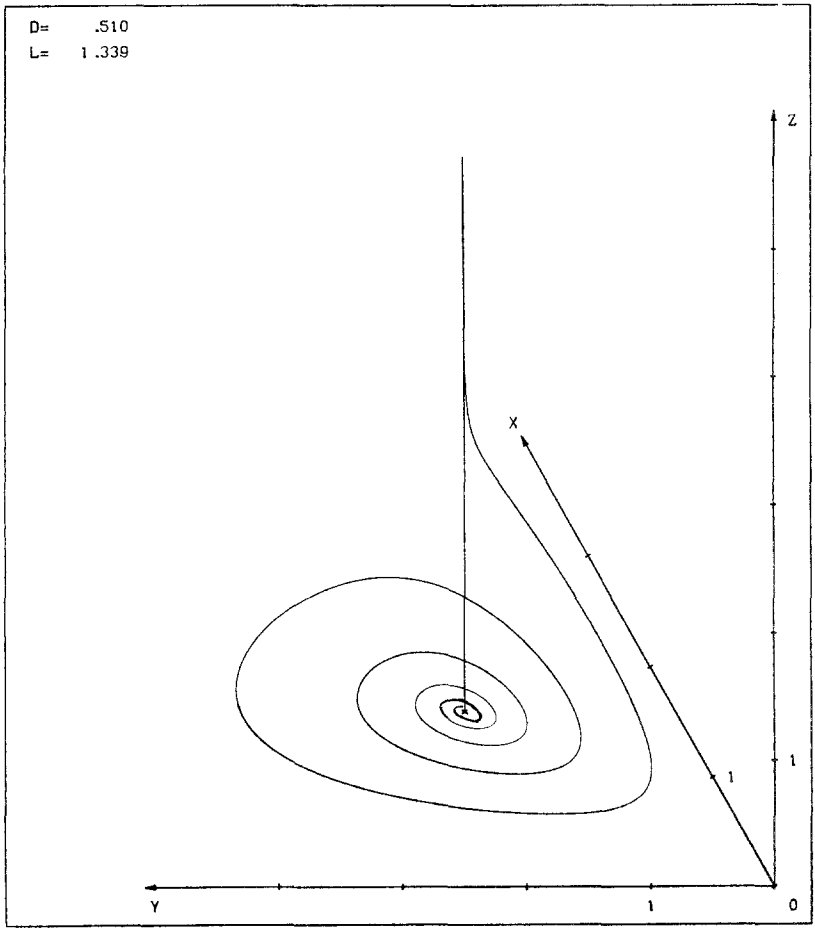

Fig. 11. Homoclinic orbit Γ_0 for model (12) around singular point (x_1, y_1, z_1), for $d = 0.510$, $l \simeq 1.339$ and other parameter values given by Eq. (17b). Eigenvalues around (x_1, y_1, z_1) are given by $(\rho \pm i\omega, \lambda)$, where $\rho \simeq 0.1311$, $\omega \simeq 1.1215$, $\lambda \simeq -332.2860$. Initial condition lies on a plane tangent to the unstable manifold at a distance of about 0.039 from the singular point, and on a plane parallel to *Oxz* passing from this latter point.

nonperiodic attractors of the type $(M^p, N^q, \ldots)$ defined above emerges, of which an example is shown in Fig. 10. The chaotic attractors observed are of the screw type, but one can expect that just above curve (b) spiral type of chaos should exist. In addition, a locus of homoclinic orbits associated to (x_1, y_1, z_1) is observed [curve (c)], whose downward tip M does not belong to curve (b). The same remark as in Rössler's model about the folding of (c) near point M arising from the folding of the unstable manifold also holds here. The corresponding homoclinic trajectory leaves the vicinity of the singular point within the two-dimensional unstable manifold of this point, visits once the upper part of the slow manifold, Eq. (14), and comes back to the singular point in the way shown in Fig. 11. As in Rössler's model, in spite of the existence of homoclinic orbits, the flow can contain periodic attractors embedded amidst the chaotic ones in parameter space.

An interesting phenomenon arises as one moves roughly along an axis parallel to l toward the locus of the homoclinic trajectory. One observes nonperiodic attractors $(1^{p_1}, \ldots, 1^{p_n})$ in which the maximum number of turns p_n of the trajectories around the singular point increases. Presumably, this reflects the fact that for the homoclinic trajectory itself the number of turns around the singular point tends to infinity.

5. DISCUSSION

We have analyzed the parameter dependence of homoclinic trajectories of two model systems involving three variables. We have shown that the onset of homoclinicity is reflected by several kinds of qualitative changes of nearby nonperiodic motions: transition from "spiral"- to "screw"-type chaos, onset of chaotic behavior with stronger mixing properties, transition to attractivity, or an increasing number of oscillations between intermittent bursts.

One question remains unanswered, namely, whether there exists any universality in some of the above-mentioned behaviors. The most promising approach to this question would be to analyze a class of equations in the vicinity of a degenerate situation like, for instance, the merging of the two singular points mentioned in Section 2. This should allow one to "see" analytically the birth of homoclinicity, and to connect this phenomenon with the onset of chaotic behavior. We intend to report on this point in a subsequent publication.

ACKNOWLEDGMENT

The research reported in this paper is supported, in part, by the U.S. Department of Energy, under contract No. DE-AS05-81ER10947.

REFERENCES

1. V. Arnold, *Chapitres supplémentaires de la théorie des equations différentielles ordinaires* (Mir, Moscow, 1980).
2. J. Guckenheimer, in *Progress in Mathematics*, Vol. 8 (Birkhäuser, Basel, 1980); P. Holmes, *S.I.A.M. J. Appl. Math.* **38**:65 (1980).
3. C. Baesens and G. Nicolis, *Z. Physik B*, submitted.
4. M. Feigenbaum, *J. Stat. Phys.* **19**:25 (1978).
5. P. Collet and J. P. Eckmann, *Iterative Maps on the Interval as Dynamical Systems* (Birkhäuser, Basel, 1981).
6. A. Arneodo, P. Coullet, and C. Tresser, *J. Stat. Phys.* **27**:171 (1982).
7. V. Afraimovitch, V. Bykov, and L. Sil'nikov, *Sov. Phys. Dokl.* **22**:253 (1977).
8. S. Smale, *Bull. Am. Math. Soc.* **73**:747 (1967).
9. A. Andronov, E. Leontovitch, I. Gordon, and A. Maier, *Theory of Bifurcations of Dynamic Systems on a Plane*, Israel program of scientific translations, Jerusalem (1971).
10. L. Sil'nikov, *Sov. Math. Dokl.* **6**:163 (1965); **10**:1368 (1969); *Math. Sbornik* **10**:91 (1970).
11. Ju. Neimark and L. Sil'nikov, *Sov. Math. Dokl.* **6**:305 (1964).
12. O. Rössler, *Ann. N.Y. Acad. Sci.* **316**:376 (1979).
13. P. Gaspard, Mémoire de Licence, University of Brussels, (1982).
14. S. Fraser and R. Kapral, *Phys. Rev. A* **25**:3223 (1982).
15. D. Farmer, J. Crutchfield, H. Froehling, N. Packard, and R. Shaw, *Ann. N.Y. Acad. Sci.* **357**:453 (1980).